International Journal of Pharmacology

Int. J. Pharmacol. **2026**; 22(2): 50132
https://doi.org/10.31083/IJP50132

Research Article

Protective Effect of Umbelliferone Against Subarachnoid Hemorrhage via Regulation of TLR2/TLR4–NF-κB–MMP-9 and PI3K/Akt Signaling Pathways

Hai Zhao[1,†], Xiaohui Liu[1,†], Yanan Zheng[1,*]

[1]Neurology Department, Baotou Central Hospital, 014040 Baotou, Inner Mongolia, China
*Correspondence: yananzheng1985@163.com (Yanan Zheng)
[†]These authors contributed equally.

Academic Editor: Mehmet Ozaslan
Submitted: 18 January 2026 Revised: 28 February 2026 Accepted: 11 March 2026 Published: 23 April 2026

Abstract

Background: Subarachnoid hemorrhage (SAH) is a cerebrovascular disease with high mortality and long-term neurological sequelae, largely driven by early brain injury, inflammation, neuronal apoptosis, and oxidative stress. Umbelliferone (7-hydroxycoumarin) exhibits notable antioxidant and anti-inflammatory properties. This study aimed to investigate the neuroprotective effect of umbelliferone in a mouse model of SAH and explore the underlying mechanisms. **Materials and Methods**: Following SAH induction, mice received the oral administration of umbelliferone (2.5, 5, or 10 mg/kg). Body weight, brain weight, and brain water content were measured to assess cerebral edema and neurological injury. Tight junction protein levels were quantified to assess blood brain barrier (BBB) integrity; meanwhile, antioxidant markers, inflammatory cytokines, and apoptosis-related parameters were also evaluated. Furthermore, mRNA expression levels in brain tissue were analyzed to elucidate the underlying molecular mechanisms. **Results**: Umbelliferone significantly improved body weight and enhanced brain weight ($p < 0.001$). Umbelliferone also altered the level of tight junction parameters (occludin, claudin-5, zonula occludens-1 (ZO-1)); oxidative stress parameters (glutathione (GSH), superoxide dismutase (SOD), catalase (CAT), glutathione peroxidase (GPx), malonaldehyde (MDA)); mitogen-activated protein kinase (MAPK) parameters (phosphorylated c-Jun N-terminal kinase(p-JNK), phosphorylated extracellular signal-regulated kinase (p-ERK), phosphorylated p38 MAPK (p-38)); inflammatory cytokines (tumor necrosis factor-α (TNF-α), interleukin-1β (IL-1β), interleukin-6 (IL-6), interleukin-18 (IL-18)); inflammatory parameters (cyclooxygenase-2 (COX-2), nuclear factor kappa B (NF-κB), transforming growth factor-β (TGF-β)); apoptosis parameters (Bcl-2-associated X protein (Bax), B-cell lymphoma 2 (Bcl-2), caspase-3, Bax/Bcl-2 ratio). Umbelliferone also significantly ($p < 0.001$) altered the mRNA expression of matrix metalloproteinase-2 (MMP-2), matrix metalloproteinase-9 (MMP-9), basigin (BSG2), TNF-α, IL-6, monocyte chemoattractant protein-1 (MCP-1), claudin-5, occludin, phosphoinositide 3-kinase (PI3K), protein kinase B (AkT), toll-like receptor 2 (TLR2) and toll-like receptor 4 (TLR4). **Conclusion**: Umbelliferone exerts neuroprotective effects against SAH in mice, at least in part, by modulating the TLR2/TLR4–NF-κB–MMP-9 and PI3K/Akt signaling pathways.

Keywords: subarachnoid hemorrhage; neuroprotection; umbelliferone; oxidative stress; apoptosis; toll-like receptor 2; nuclear factor-kappa B; matrix metalloproteinase 9

1. Introduction

Early brain injury (EBI), following subarachnoid hemorrhage (SAH) shows a complex cascade of cellular and molecular events that progress beyond the primary mechanical insult, which contributes to secondary neuronal injury and neurological dysfunction [1]. The quick enhancement in intracranial pressure and the resultant cerebral hypoperfusion initiate a series of events that disrupt blood brain barrier (BBB) homeostasis, ultimately leading to vasogenic edema and subsequent influx of proinflammatory mediators [2,3]. Neuroinflammation, driven by activated microglia and immune cell infiltration, exacerbates tissue damage by releasing pro-inflammatory mediators, including cytokines and chemokines. Mitochondrial dysfunction further aggravates the cellular energy deficit and activates apoptotic cascades, establishing a vicious cycle that amplifies neuronal degeneration. The pathophysiological environment in the brain is very complex, as it not only compromises immediate neuronal survival but also predisposes the brain to delayed complications like cerebral vasospasm and ischemia [4–6]. Apoptosis, a tightly regulated form of programmed cell death, plays a critical pathophysiological role in EBI and largely determines the extent of glial and neuronal cell loss after SAH. Cellular degradation and DNA fragmentation are mediated by caspases, which are activated through both intrinsic and extrinsic apoptotic pathways. Modulation of these apoptotic pathways has been shown to significantly affect the progression of brain injury in experimental models; therefore, apoptosis has emerged as a promising therapeutic target for the treatment of SAH. The preclinical studies suggest that pharmacological compounds that block major intracellular apoptotic cascades (e.g., caspase inhibitors, mitochondrial membrane stabilisers) are effective in suppressing brain edema and improv-

ing functional outcome. Preliminary clinical trials investigating anti-apoptotic therapies have demonstrated promising neuroprotective potential, but more research needs to be required to scrutinize the initiating molecular mechanisms and to determine the optimal timing for potential intervention [1,6,7]. Apoptosis-targeted treatments may transform the current therapeutic paradigm for SAH, shifting the focus from merely preventing re-rupture to actively amelioration of early neuronal injury, and improving the long-term neurological complications.

Secondary complications after SAH, such as brain edema, BBB permeability disruption, neuronal cell apoptosis, and cerebral vasospasm (CVS) are sequential pathophysiological events that have important roles in the prognosis of SAH in patients. These complications are, in part, facilitated by biochemical dysregulation, including oxidative stress, increased inflammation, and toxic metabolite accumulation [1,3]. Oxidative stress is a major contributor to cellular damage and enhances neuroinflammation, compromising neuronal survival and vascular stability. The interactive effects of these factors result in a vicious cycle that aggravates brain injury and hinders recovery following SAH. Recently, activation of nuclear factor erythroid 2-related factor 2 (Nrf2) was considered as an essential mediator in the amelioration of these secondary injuries through coordinating cellular protective responses against oxidative and inflammatory insults [8]. This involves the cytoplasmic retention of Nrf2 by its repressor, kelch-like ECH-associated protein 1 (Keap1), under basal conditions. Under resting conditions, Nrf2 is sequestered by its negative regulator, Keap1, which retains the transcription factor in the cytoplasm for degradation via the ubiquitin-proteasome pathway. But under oxidative or xenobiotic stimuli, Nrf2 dissociates from its tether to the Keap1 complex and translocates to the nucleus, where it induces the transcription of antioxidant response element (ARE) genes, thereby controlling the expression of antioxidant and detoxifying enzymes. In fact, studies in experimental models of CNS injury demonstrate that Nrf2 deficiency exacerbates neural injury, whereas pharmacological induction of Nrf2 with agents such as tert-butylhydroquinone (tBHQ) or sulforaphane results in neuroprotection [9–11]. However, the exact mechanisms of Nrf2 activation and its potential therapies for SAH remain poorly understood, despite positive results in other CNS injuries; thus, more studies are needed to elucidate the underlying mechanisms and refine targeted intervention strategies.

The Bcl-2/Bax/Cleaved caspase-3 signaling pathway plays a significant role in the regulation of intrinsic apoptotic pathways, especially mitochondrial dysfunction, which is considered to have an integral role in several nervous system diseases [12]. Bcl-2 is an anti-apoptotic protein that maintains mitochondrial integrity, and Bax promotes apoptosis by inducing the breakdown of the mitochondrial outer membrane and activating downstream effectors such as cleaved caspase-3, resulting in cell death. Dysfunction of such a pathway may thus participate in pathological neuronal death, and has been involved in disorders, for instance, neurodegenerative diseases, ischemic insults or SAH [13,14]. Among the sirtuins, Sirt3 is a mitochondrial NAD(+)-dependent deacetylase that protects against oxidative stress by modulating the activity of antioxidant enzymes, including superoxide dismutase 2 (SOD2). Sirt3 expression in cortical neurons is downregulated in a time-dependent manner after SAH, in parallel with SOD2 levels, suggesting that it plays an important role as an antioxidant factor that attenuates oxidative damage following hemorrhage. This decrease in Sirt3 may further enhance mitochondrial dysfunction and apoptosis by decreasing the cell's level of reactive oxygen species scavenging, resulting in the augmentation of neuronal injury [14,15]. Therefore, Sirt3 and its downstream signaling might be good targets for treatment to increase neuronal survival in SAH and other oxidative stress-related central nervous system diseases.

Umbelliferone (UF), or 7-hydroxycoumarin, is a derivative of coumarin, and a type of phenylpropanoid. It forms colourless crystals with a characteristic odor reminiscent of vanilla [16]. It is known for its unique chemical structure, which contains a benzopyrone core featuring a hydroxyl group at the seventh position. It has been shown that 5-(Tetradecyloxy)-2-furoic acid (TOFA) has anti-inflammatory, antimicrobial and anticancer activities, which make it as a potential therapeutic agent [17–19]. In this experimental study, we explore the neuroprotective effect of UF against SAH in mice and explore the underlying mechanism.

2. Material and Method

2.1 Experimental Mice

In this experimental study, we used the C57BL/6 mice (sex: male; aged: 8–10 weeks and weight: 25–30 g). The mice were received by the department's animal house and kept in single cages. The mice were kept in standard laboratory conditions (22 $\pm$ 2 °C; 60–70% relative humidity; 12 h/12 h light/dark cycle) and had free access to water and food. The experimental protocols were reviewed and approved by the Animal Ethics Committee of and all procedures were performed under the approved ethical standards. The ethics approval number is [Approval No. 12783948].

Animals were anesthetized using pentobarbital sodium administered intraperitoneally at a dose of 50 mg/kg body weight (10 mg/mL solution prepared in sterile normal saline). Adequate depth of anesthesia was confirmed by the absence of pedal withdrawal and corneal reflexes before any experimental procedures were initiated. At the end of the experiment, animals were euthanized under deep anesthesia using an overdose of pentobarbital sodium ($\geq$150 mg/kg, intraperitoneally). Death was confirmed by cessation of respiration and heartbeat,

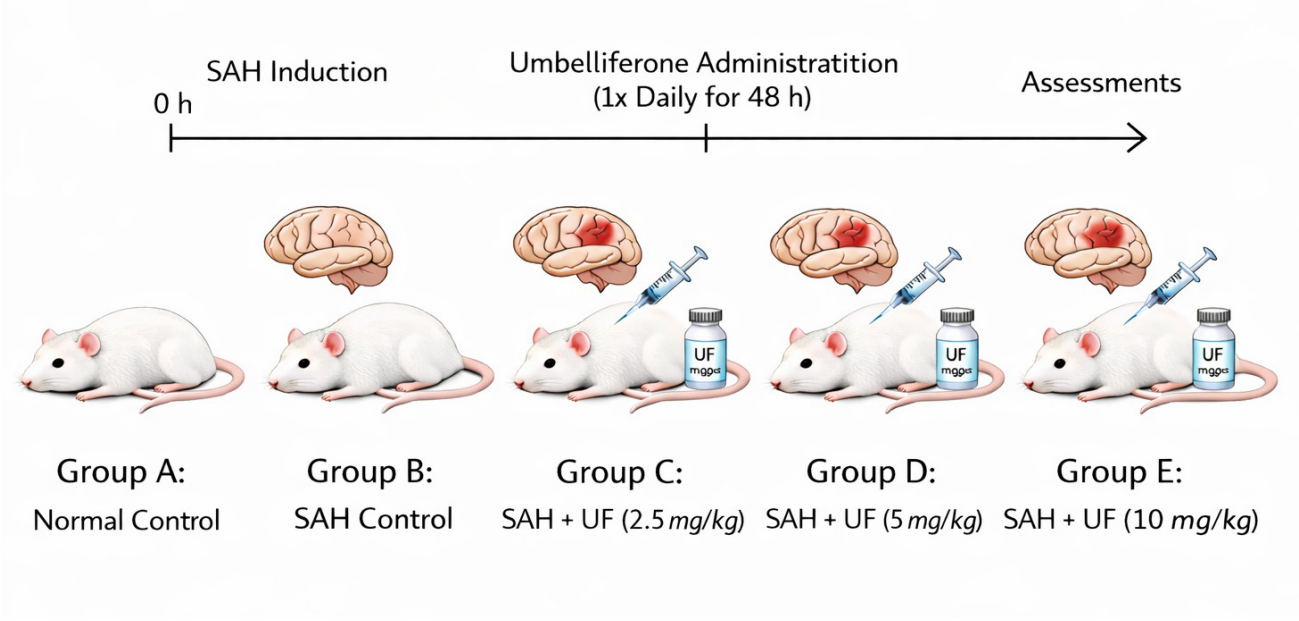

Fig. 1. Experimental group. SAH, subarachnoid haemorrhage; UF, umbelliferone.

followed by cervical dislocation to ensure irreversibility. These procedures were performed in accordance with the Regulations on the Administration of Laboratory Animals of the People's Republic of China and internationally accepted animal welfare guidelines.

2.2 SAH Model

Mice were induced under SAH using the previously reported method [12]. In short, the mice were anesthetized with pentobarbital sodium (50 mg/kg) and the rectal temperature was maintained using a heat blanket (37 ± 0.5 °C). We exposed the carotid arteries (internal, external, and common), then ligated and cut the left external carotid artery, leaving an arterial stump measuring 3 mm. Using a nylon suture, the left side was accessed through the branch of the middle cerebral artery and advanced approximately 3–5 mm into the lumen of the artery. SAH was constructed for 10 s. Normal control mice were similarly treated, except their blood vessels were not pricked, and there was no significant change in the blood flow. We tracked changes in blood flow before and after vessel puncture in all mice. After the operation, the mice were returned to their cages to recover.

2.3 Drug Preparation

Umbelliferone (98%, Sigma-Aldrich) was purchased and administered to the mice as an oral suspension. Firstly, prepare the oral suspension by dissolving the tested drug in 1% carboxymethylcellulose (CMC).

2.4 Experimental Group

After the induction of SAH, the mice were divided into the following groups (n = 10), and the experimental group is shown in Fig. 1. Animals were subsequently divided into subgroups after SAH induction and randomization (n = 10 per group) to facilitate proper tissue processing. For neurological evaluation and naloxone administration (wet–dry) measurement, five mice per group were used, while another five mice were used for biochemical and molecular analysis. For the ELISA and qRT-PCR assays, the ipsilateral cerebral cortex was meticulously dissected at 4 °C, half were homogenized for protein estimation, while the neighbouring cortical area was flash-frozen in liquid nitrogen and stored at –80 °C until further analysis of mRNA expression.

After isolating the ipsilateral cortical tissues, they were lysed in ice-cold lysis buffer RIPA containing proteases and phosphatase inhibitors (Thermo Fisher Scientific, Waltham, MA, USA) followed by centrifugation at 12,000 rpm for 15 min at 4 °C. The supernatant was retrieved and protein concentration was determined with BCA protein assay kit (Thermo Fisher Scientific).

2.5 SAH Grade

For the estimation of SAH grade, the high-resolution images of the blood clots in the basal cisterns [12]. As per the score system, the following groups and their scores:

Mild SAH: 0–7 points,

Moderate SAH: 8–12 points, and

Severe SAH: 13–18 points.

2.6 Neurological Score

All mice in each group were assessed for neurological performance using the modified Garcia scale and Rotarod test following 48 h post-SAH period. The symmetry movements of limbs, spontaneous activity, climbing, forepaw outstretching, tentacle reaction and body proprio-

Table 1. List of primers.

S. No	Genes	Primer (5′- 3′)	
		Forward	Reverse
1	*CLDN5*	TAAGGCACGGGTGGCACTCA	CTACGATGTTGGCGAACCAG
2	*BSG2*	GTTTGTGAAGCTGATCTGCAAG	ACAGCTCAGGCGTGGATATAAT
3	*OCLN*	TAGCCATTGTCCTGGGGTTCAT	TTTCTTCGGGTTTTCACAGCAAA
4	*TNF-α*	AAGCATGATCCGAGATGTGGAACTG	CGCCACGAGCAGGAATGAGAAG
5	*IL-6*	ACTTCCAGCCAGTTGCCTTCTTG	TGGTCTGTTGTGGGTGGTATCCTC
6	*MCP-1*	CTCACCTGCTGTACTCATTCACTG	CTTCTTTGGGACACCTGCTGCTG
7	*MMP-2*	GCAACCACAACCAACTACGA	CCAGTGTCAGTATCAGCATCAG
8	*MMP-9*	GCAAACCCTGCGTATTTCCAT	CCATCCGAGCGACCTTTAGTG
9	*PI3K*	GCTGGACTTGGTGTTGAAGA	GGATGTAGCCATCAGGTTGA
10	*Akt*	TGGACTACATGAGCGACAAG	GGTGCCGTAGTCATCCATAA
11	*TLR2*	GCTTTCCTGCTCAACTTCCT	TGGTCATCTTGGGCTTCTTC
12	*TLR4*	GGACTCTGAATCGGAGGAAA	CCAAGTCTCTGAAGGGTCTG
13	*GAPDH*	TGGAAAGCTGTGGCGTGAT	AACGGATACATTGGGGGTAG

ception were assessed by following the previously reported literature by Garcia *et al*. [20]. For the rotarod test, we measured the performance of all mice before surgery (1 day) and 48 h post-SAH. To summarize, the mice were placed on a cylinder, and the rotation rate was increased from 4 to 40 rpm for 5 minutes. As reported earlier [21], the latency to falling off in three consecutive trials was calculated.

2.7 Brain Edema

For the estimation of brain edema, we estimated the brain water level in the all-group mice. Briefly, after the surgery, the brains were immediately removed (48 h) and the brain tissue was quickly divided into four parts, such as the hemisphere (right and left), the brain stem, and the cerebellum. Each part was weighed quickly to get the wet weight and dried in a 100 °C for 24 h using the oven to get dry weight. The brain water level was estimated using the following formula [21]:

$$\text{brain water content}\ (\%) = \frac{(\ \text{Wet weight}\ -\ \text{Dry weight}\ )}{\text{Wet weight}} \times 100$$

2.8 Biochemical Parameters

The antioxidant parameters such as MDA (Cat. No: E-BC-K025-M), GSH (Cat. No: E-BC-K030-M), GPx (Cat. No: E-BC-K096-M), CAT (Cat. No: E-BC-K031-M) and SOD (Cat. No: E-BC-K020-M); inflammatory cytokines include TNF-α (Cat. No: E-EL-M0049), IL-1β (Cat. No: E-EL-M0037), IL-6 (Cat. No: E-EL-M0044), IL-18 (Cat. No: E-EL-M0730); inflammatory parameters include COX-2 (Cat. No: E-EL-M0959), NF-κB (Cat. No: E-EL-M0054), TGF-β (Cat. No: E-EL-M0055); apoptosis parameters viz., Bax (Cat. No: E-EL-M0007), Bcl-2 (Cat. No: E-EL-M0008) and caspase-3 (Cat. No: E-EL-M0033) were estimated using the ELISA kit following the manufacture instruction (Elabscience Biotechnology Inc., Wuhan, China).

Commercially available ELISA kits were used to determine the protein amounts of ERK (Cat. No. E-EL-R2665), JNK (Cat. No. E-EL-R2406), p38 (Cat. No. E-EL-R2536) and their phosphorylated forms (p-ERK, p-JNK, and p-p38) according to manufacturer's instructions with equal amounts of total proteins (Elabscience Biotechnology Inc., Wuhan, China).

2.9 Quantitative Real-Time PCR

After the experimental phase, all the mice were sacrificed and their cortex was immediately frozen on dry ice and stored in RNA buffer until the mRNA isolation protocol. mRNA was isolated using the Total RNA Mini Kit (A&A Biotechnology, Poland) according to the manufacturer's instructions. Reverse transcription was conducted at 100 ng/µL using the NG dART RT Kit in a DNA Engine DNA thermocycler. mRNA expression was assessed by quantitative real-time PCR in a standard mode using the SYBR Green Master Mix and primers listed in Table 1. GAPDH served as the internal standard.

2.10 Statistical Analysis

Values are presented as the mean and standard deviation (SD). The statistical analyses were performed with GraphPad Prism (version 8; GraphPad Software, San Diego, CA, USA). Data normality was first checked by the Shapiro-Wilk. Comparisons between more than two groups were performed using one-way ANOVA followed by Tukey's multiple comparisons test. Two-group comparisons were done using an unpaired Student's *t*-test. Statistical significance was considered at $p < 0.05$.

3. Result

3.1 Body Weight and Brain Weight

SAH group mice exhibited reduced body weight, brain damage, and increased brain water content compared with

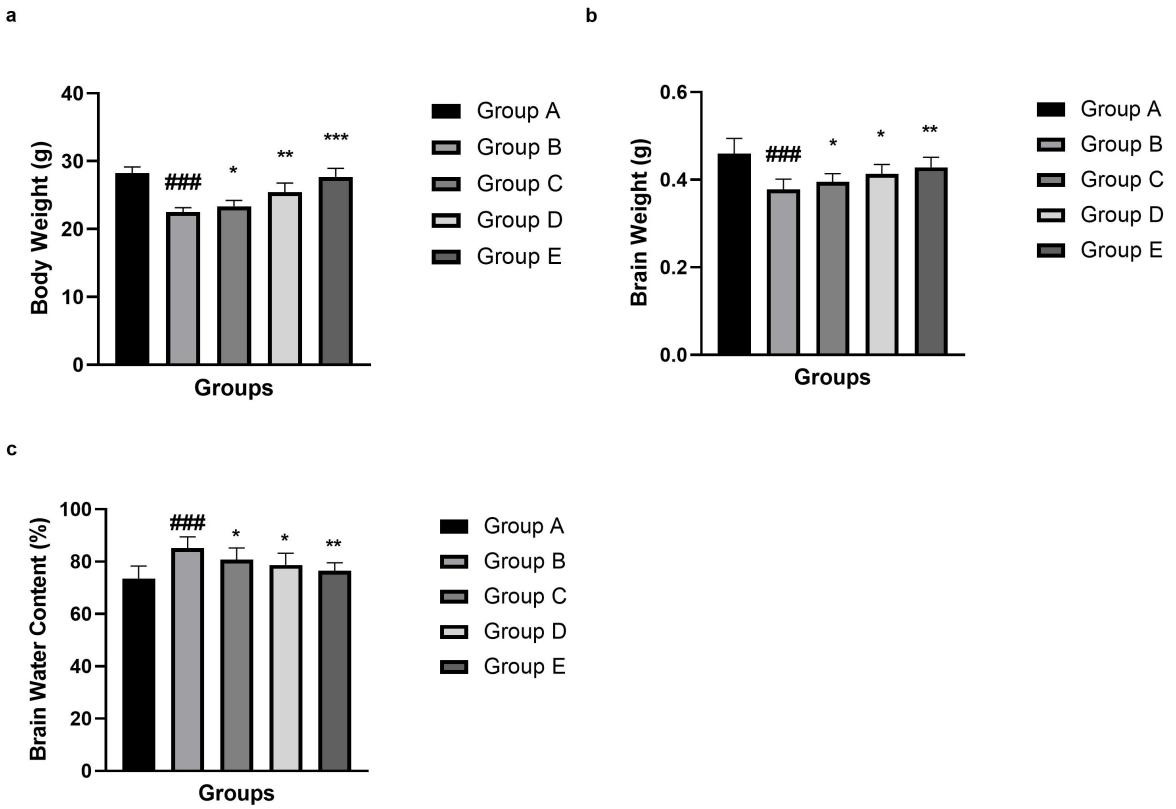

Fig. 2. Effect of umbelliferone on the body weight, brain weight and brain water content against SAH in mice. (a) body weight, (b) brain weight and (c) brain water content. Data are presented as the mean ± standard deviation (SD), with ten mice in each group. $^{###}p < 0.001$ SAH vs normal control; $^{*}p < 0.05$, $^{**}p < 0.01$ and $^{***}p < 0.001$ compared umbelliferone group vs SAH.

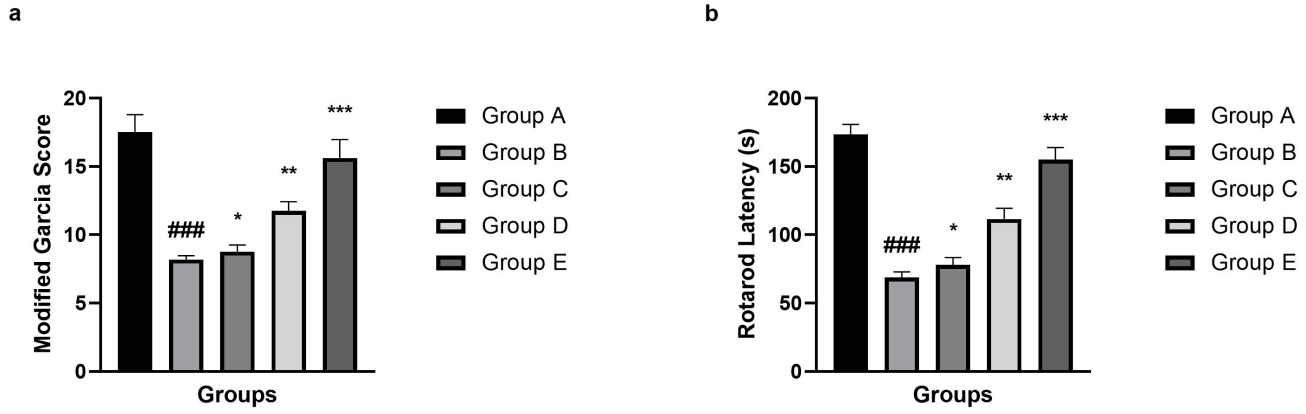

Fig. 3. Effect of umbelliferone on the modified Garcia Score and Rotarod latency against SAH in mice. (a) Modified Garcia Score and (b) Rotarod latency. Data are presented as the mean ± SD, with ten mice in each group. $^{###}p < 0.001$ SAH vs normal control; $^{*}p < 0.05$, $^{**}p < 0.01$ and $^{***}p < 0.001$ compared umbelliferone group vs SAH.

the normal control group. Umbelliferone treatment significantly ($p < 0.001$) improved the body weight (Fig. 2a), brain weight (Fig. 2b) and brain water content (Fig. 2c).

3.2 Neurological Parameters

SAH group mice showed a suppressed modified Garcia Score (Fig. 3a) and Rotarod latency (Fig. 3b) as compared to the normal control group mice. Umbelliferone treatment significantly ($p < 0.001$) improved the modified Garcia Score and Rotarod Latency at dose dependent manner.

3.3 SAH Assessment

The NC group displayed no signs of blood loss (score = 0). In all groups of SAH-induced models, the magnitude of haemorrhage was relatively consistent. The mean score

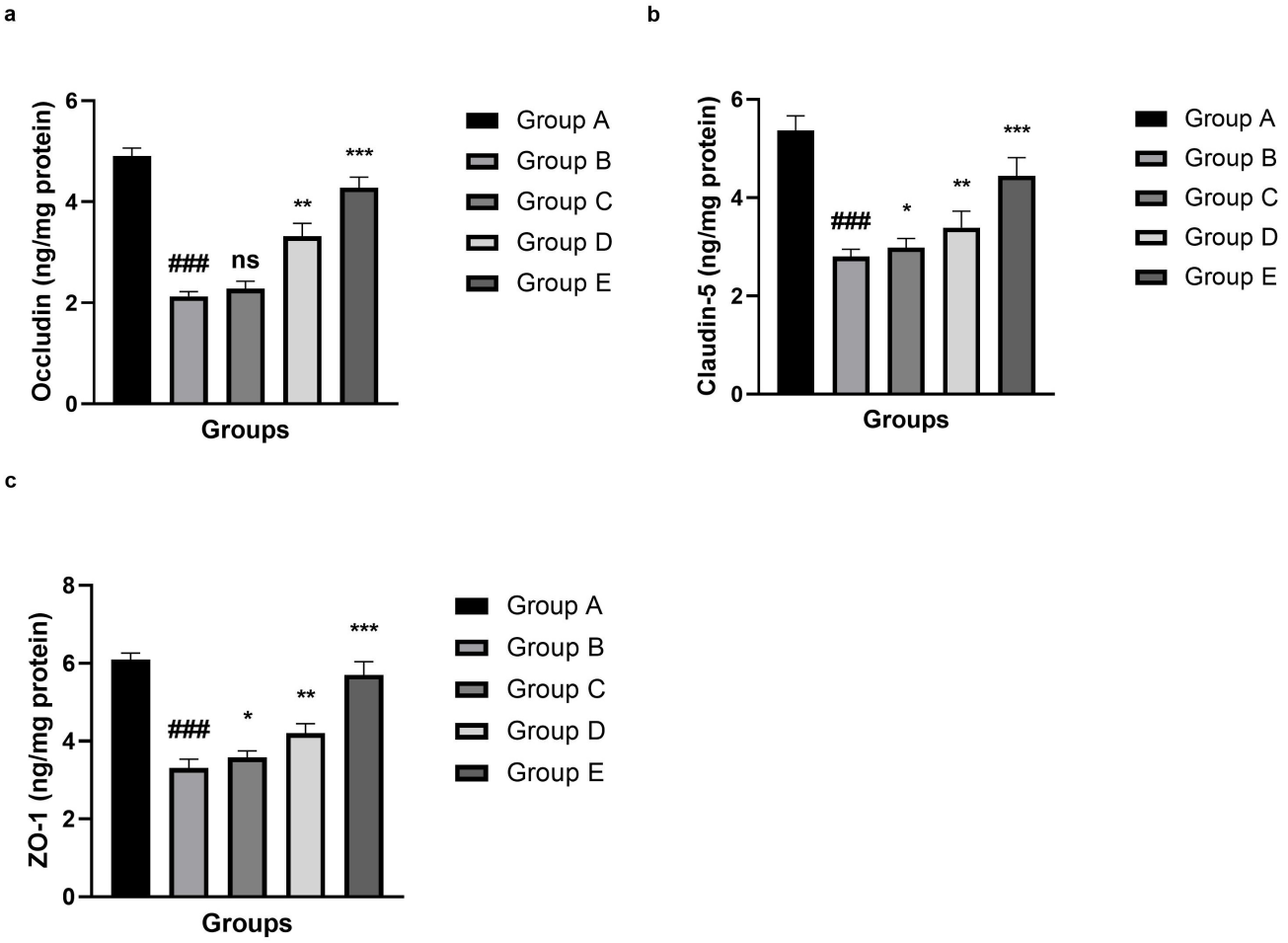

Fig. 4. Effect of umbelliferone on the tight junction parameter against SAH in mice. (a) Occludin, (b) claudin-5 and (c) ZO-1. Data are presented as the mean ± SD, with ten mice in each group. ns, not significant; $^{###}p < 0.001$ SAH vs normal control; $^{*}p < 0.05$, $^{**}p < 0.01$ and $^{***}p < 0.001$ compared umbelliferone group vs SAH. ZO-1, zonula occludens-1.

Table 2. SAH Grade Scores in Experimental Groups.

S. No	Group	Groups	SAH Grade Score
1	A	NC (Normal Control)	0
2	B	SAH	$12.8 \pm 0.6^{###}$
3	C	SAH + Umbelliferone (2.5 mg/kg)	11.1 ± 0.5*
4	D	SAH + Umbelliferone (5 mg/kg)	8.6 ± 0.8**
5	E	SAH + Umbelliferone (10 mg/kg)	5.4 ± 0.3***

Data are presented as the mean ± SD, with ten mice in each group. $^{###}p < 0.001$ SAH vs normal control; $^{*}p < 0.05$, $^{**}p < 0.01$ and $^{***}p < 0.001$ compared umbelliferone group vs SAH. SAH, subarachnoid haemorrhage.

of SAH grade in SAH group was 12.8 ± 0.6, compared with SAH + UM (2.5 mg/kg), SAH + UM (5 mg/kg) and SAH + UM (10 mg/kg) groups that had scores of 11.1 ± 0.5, 8.6 ± 0.8 and 5.4 ± 0.3, respectively (Table 2). These results verify that baseline hemorrhage volume was similar in the entire SAH group before treatment, and are not affected by differences between the initial grade of SAH on the therapeutic causative effects of umbelliferone.

3.4 Tight Junction Parameter

The results showed that the integrity of the BBB was seriously compromised after SAH, which manifested as a significant ($p < 0.001$) decrease of tight junction proteins such as occludin (Fig. 4a), claudin-5 (Fig. 4b) and zonula occludens-1 (ZO-1) (Fig. 4c) in Group B when compared to the normal control (Group A). Occludin levels were significantly decreased in the SAH control group. Similarly, Fig. 4b indicated that the level of claudin-5 was significantly ($p < 0.001$) reduced after SAH and gradually increased with UF treatment. Consistent with these results, Fig. 4c demonstrated a marked reduction in ZO-1 level for Group B that was evidently counteracted by Groups C, D, and E, in a dose-dependent manner.

3.5 Antioxidant Parameters

The results indicated a marked abnormality in the oxidative stress status after SAH induction, as demonstrated in Fig. 5. Endogenous antioxidant defenses were significantly altered ($p < 0.001$) in comparison with the normal control group (Group A), as evidenced by modulated levels

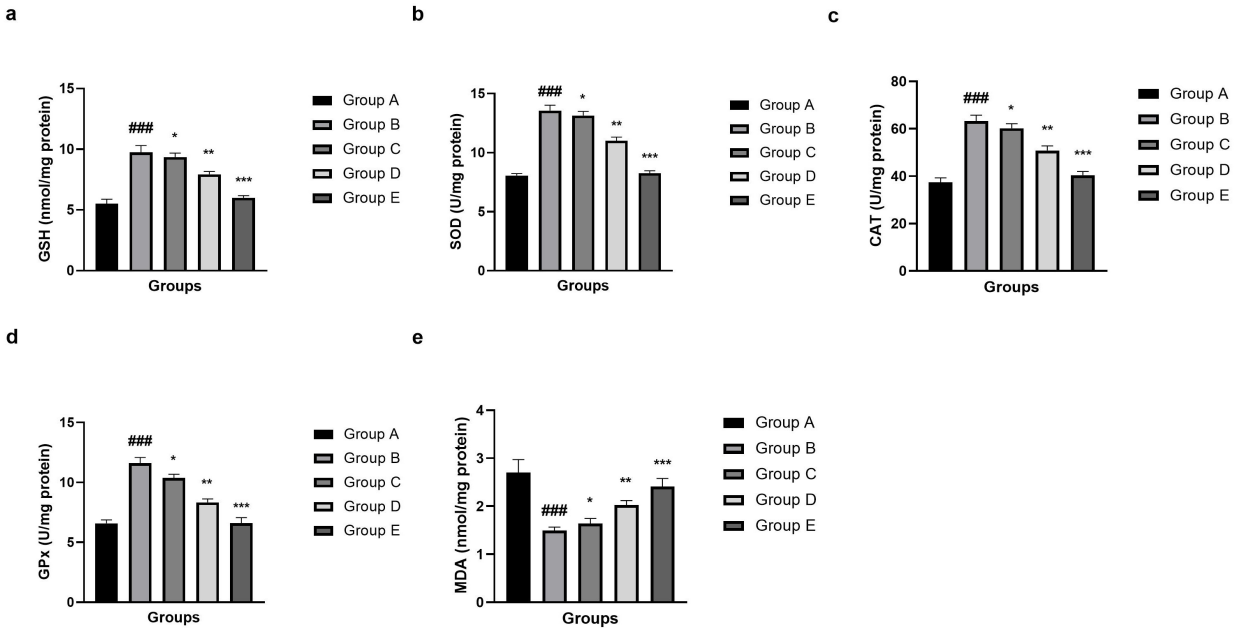

Fig. 5. Effect of umbelliferone on the oxidative stress parameters against SAH in mice. (a) GSH, (b) superoxide dismutase (SOD), (c) CAT, (d) GPx and (e) MDA. Data are presented as the mean ± SD, with ten mice in each group. $^{###}p < 0.001$ SAH vs normal control; $^{*}p < 0.05$, $^{**}p < 0.01$ and $^{***}p < 0.001$ compared umbelliferone group vs SAH. GSH, glutathione; CAT, catalase; GPx, glutathione peroxidase; MDA, malonaldehyde.

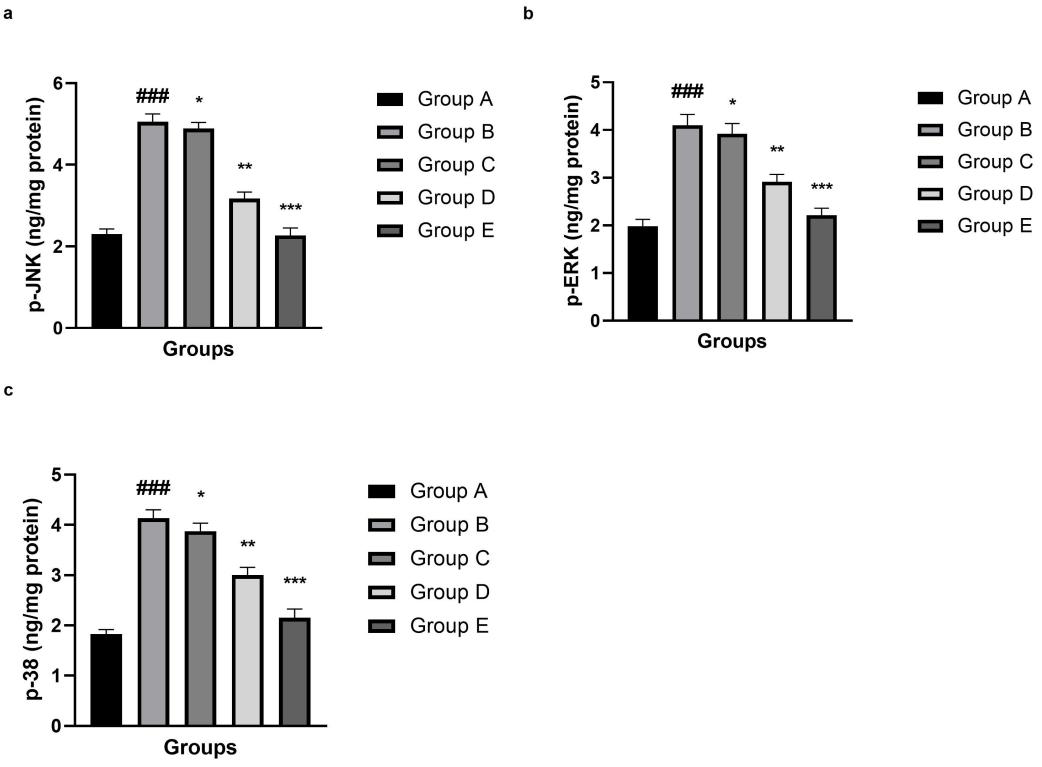

Fig. 6. Effect of umbelliferone on the MAPK parameter against SAH in mice. (a) p-JNK, (b) p-ERK and (c) p-38. Data are presented as the mean ± SD, with ten mice in each group. $^{###}p < 0.001$ SAH vs normal control; $^{*}p < 0.05$, $^{**}p < 0.01$ and $^{***}p < 0.001$ compared umbelliferone group vs SAH. MAPK, mitogen-activated protein kinase; p-ERK, phosphorylated extracellular signal-regulated kinase; p-JNK, phosphorylated c-Jun N-terminal kinase; p-38, phosphorylated p38 MAPK.

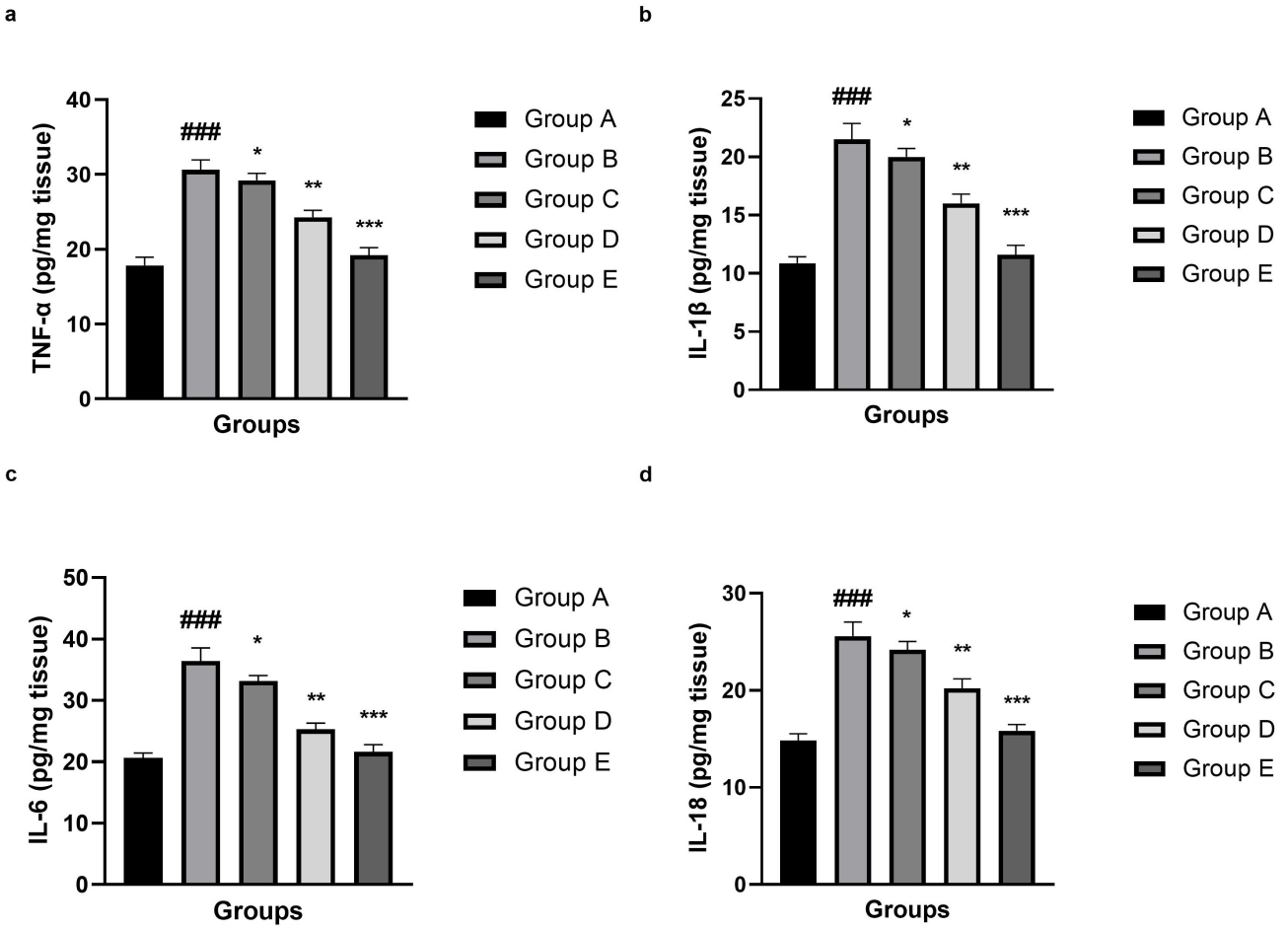

Fig. 7. Effect of umbelliferone on the inflammatory cytokine parameters against SAH in mice. (a) TNF-α, (b) IL-1β, (c) IL-6 and (d) IL-18. Data are presented as the mean $\pm$ SD, with ten mice in each group. $^{\#\#\#}p < 0.001$ SAH vs normal control; $^{*}p < 0.05$, $^{**}p < 0.01$ and $^{***}p < 0.001$ compared umbelliferone group vs SAH. TNF-α, tumor necrosis factor-α; IL-1β, interleukin-1β.

of GSH (Fig. 5a), SOD (Fig. 5b), CAT (Fig. 5c) and GPx (Fig. 5d), along with a significant altered in MDA levels (Fig. 5e), indicating enhanced lipid peroxidation.

3.6 MAPK Parameters

The findings revealed a prominent induction of the mitogen-activated protein kinase (MAPK) signalling pathway after SAH. The level of phosphorylation of JNK (Fig. 6a), ERK (Fig. 6b), and p38 (Fig. 6c) was significantly ($p < 0.001$) enhanced in Group B compared to those in Group A. This activation was markedly ($p < 0.001$) suppressed by UF in a dose-related manner.

3.7 Inflammatory Cytokines and Parameters

Compared with the normal control (Group A), significant ($p < 0.001$) increases in TNF-α (Fig. 7a), IL-1β (Fig. 7b), IL-6 (Fig. 7c) and IL-18 (Fig. 7d) levels were observed in Group B and marked upregulation of COX-2 (Fig. 8a), NF-κB (Fig. 8b) and TGF-β (Fig. 8c) levels, suggesting that inflammatory curiosity occurs after SAH. These inflammatory changes were markedly diminished by the treatment of UF in a dose-dependent manner. These results suggest that UF possesses potent anti-inflammatory power and attenuates SAH-induced neuroinflammation by inhibiting cytokine release and critical inflammatory signaling pathways.

3.8 Apoptosis Parameters

The result revealed an obvious upregulation of mitochondrial-dependent apoptosis after SAH onset. As illustrated in Fig. 9a–d, pro-apoptotic parameters were significantly ($p < 0.001$) augmented, whereas anti-apoptotic protein (Bcl-2) was decreased, compared with normal control mice (Group A). These studies show increased neuronal apoptotic signaling following SAH. UF treatment dramatically ($p < 0.001$) reduced changes in apoptosis.

3.9 mRNA Expression

Gene expression experiments revealed significant changes in inflammatory, matrix-degrading and blood–brain barrier-related genes during SAH. As shown in Fig. 10, there was a significant increase of mRNA levels

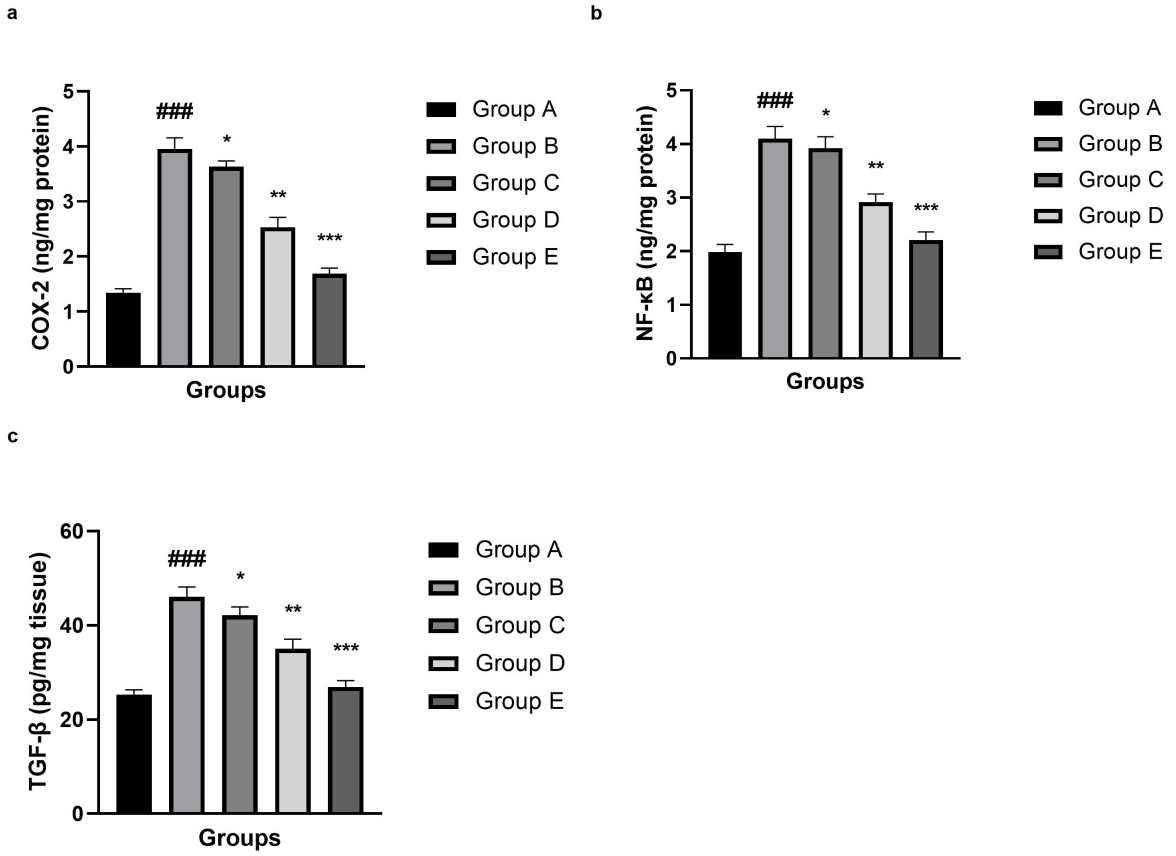

Fig. 8. Effect of umbelliferone on the inflammatory parameters against SAH in mice. (a) COX-2, (b) NF-κB and (c) TGF-β. Data are presented as the mean $\pm$ SD, with ten mice in each group. $^{\#\#\#}p < 0.001$ SAH vs normal control; $^{*}p < 0.05$, $^{**}p < 0.01$ and $^{***}p < 0.001$ compared umbelliferone group vs SAH. COX-2, cyclooxygenase-2; NF-κB, nuclear factor kappa B; TGF-β, transforming growth factor-β.

of MMP-2 (Fig. 10a), MMP-9 (Fig. 10b), BSG2 (Fig. 10c), TNF-α (Fig. 10d), IL-6 (Fig. 10e), MCP-1 (Fig. 10f) and reduce claudin-5 (Fig. 10g), occludin (Fig. 10h) in Group B (SAH control group) compared with that in Group A, indicating more severe neuroinflammation and ECMs degradation. The expression of these genes was significantly ($p < 0.001$) down-regulated by UF.

This analysis revealed that the mRNA expression of PI3K (Fig. 11a), Akt (Fig. 11b), TLR2 (Fig. 11c) and TLR4 (Fig. 11d) varied significantly ($p < 0.001$) among the experimental groups. The expression of PI3K and Akt mRNA was significantly ($p < 0.001$) decreased in Group B vs the normal control (Group A) after SAH. Treatment with UF dose-dependently reversed the expression levels.

4. Discussion

Neuroinflammation is a key factor in secondary brain injury and poor outcomes in patients with SAH. Natural products with antioxidant and anti-inflammatory properties have gained attention as potential treatments for these damaging processes. Umbelliferone may reduce oxidative stress and the inflammatory cascade triggered by SAH and could help protect neurological tissue from damage [1,2]. However, the exact mechanism through which umbelliferone influences SAH-induced neuroinflammation has not yet been fully determined. It may also be valuable to investigate whether umbelliferone's effects are mediated by main molecular targets involved in post-SAH inflammatory responses, such as microglial activation, cytokine release, and BBB permeability [2,3] Umbelliferone is a free radical scavenger, possessing strong antioxidant activities which are ascribed to its ability to inhibit xanthine oxidases and metal chelating properties. These features indicate that umbelliferone may inhibit oxidative stress and the inflammatory cascade induced by SAH, and may help protect neurological tissue from damage. However, the exact mechanism by which umbelliferone exerts its effects on SAH-induced neuroinflammation has yet to be fully elucidated. It might be also interesting to validate whether the umbelliferone action is mediated via main molecular targets associated with post-SAH inflammatory responses, such as microglial activation, cytokine release and blood-brain barrier (BBB) permeability [1,3,6]. In the present study, we aim to clarify these mechanisms by discussing current evidence on umbelliferone's effects on inflammatory mediators and oxidative stress markers in SAH, as well as laying a solid

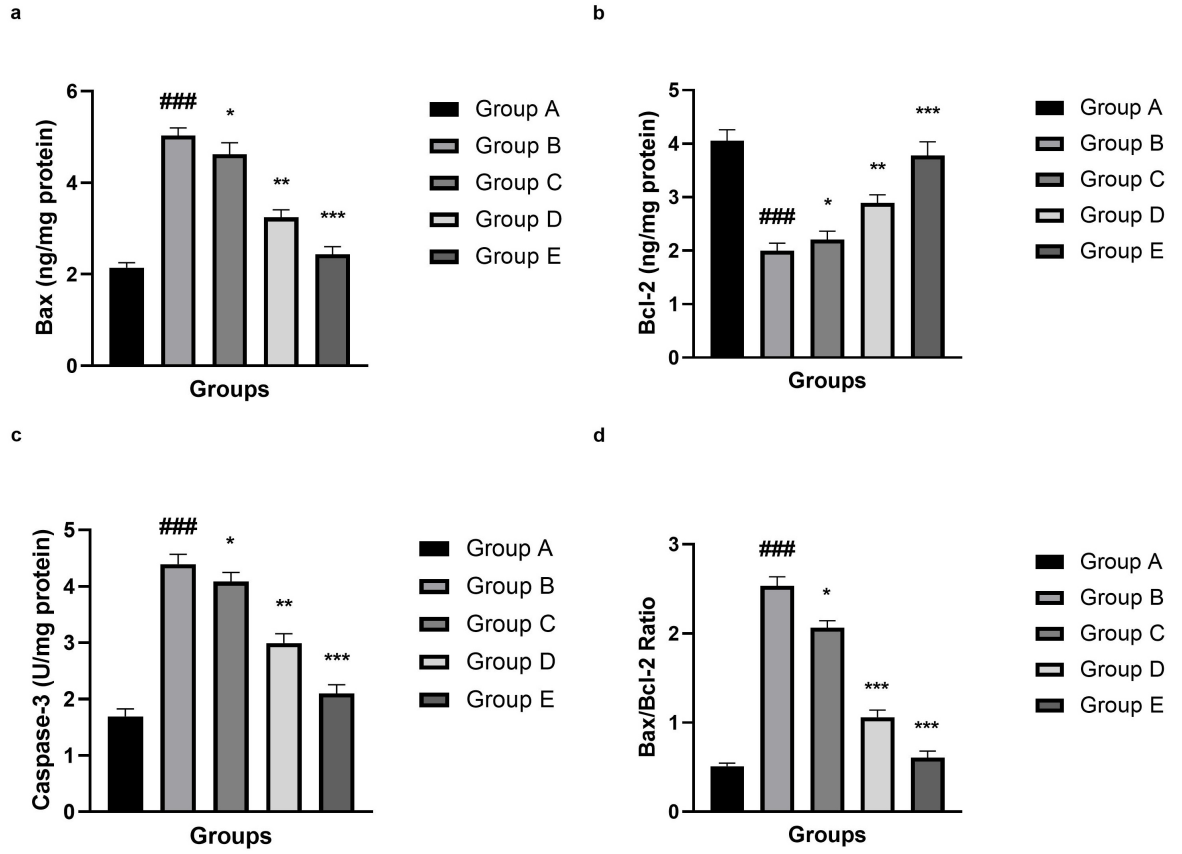

Fig. 9. Effect of umbelliferone on the apoptosis parameters against SAH in mice. (a) Bax, (b) Bcl-2, (c) caspase-3 and (d) Bax/Bcl-2 ratio. Data are presented as the mean ± SD, with ten mice in each group. $^{###}p < 0.001$ SAH vs normal control; $^{*}p < 0.05$, $^{**}p < 0.01$ and $^{***}p < 0.001$ compared umbelliferone group vs SAH. Bax, Bcl-2-associated X protein; Bcl-2, B-cell lymphoma 2.

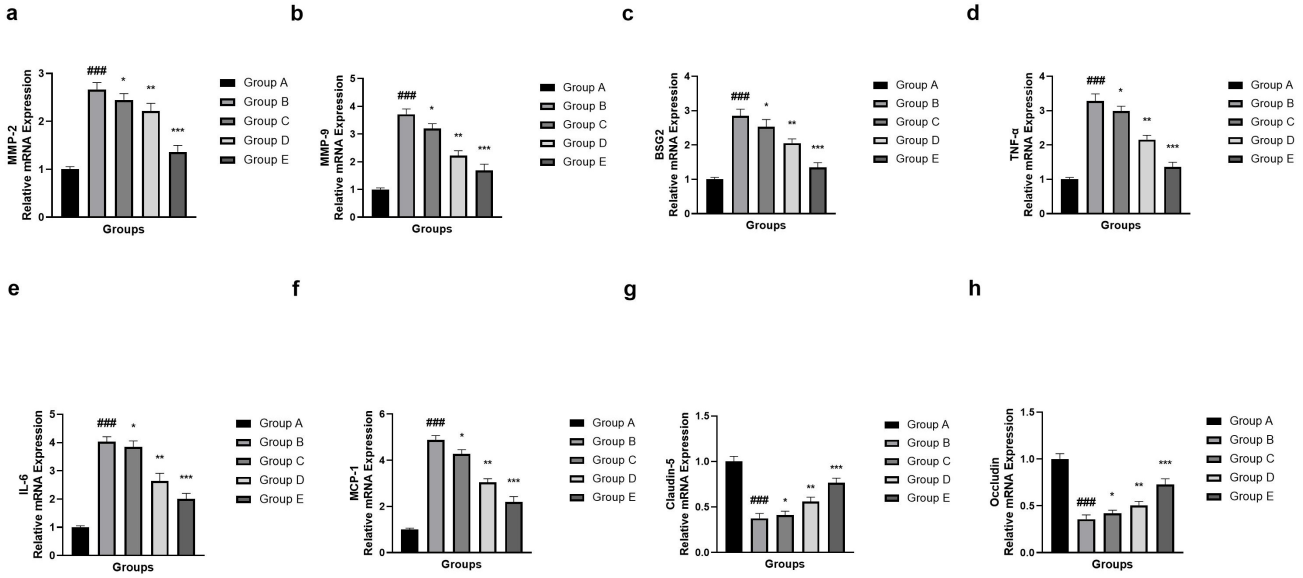

Fig. 10. Effect of umbelliferone on the mRNA expression (MMP-2, MMP-9, BSG2, TNF-α, IL-6, MCP-1, claudin-5 and occludin) against SAH in mice. (a) MMP-2, (b) MMP-9, (c) BSG2, (d) TNF-α, (e) IL-6, (f) MCP-1, (g) claudin-5 and (h) occludin. Data are presented as the mean ± SD, with ten mice in each group. $^{###}p < 0.001$ SAH vs normal control; $^{*}p < 0.05$, $^{**}p < 0.01$ and $^{***}p < 0.001$ compared umbelliferone group vs SAH. MMP-2, matrix metalloproteinase-2; MMP-9, matrix metalloproteinase-9; BSG2, basigin; MCP-1, monocyte chemoattractant protein-1.

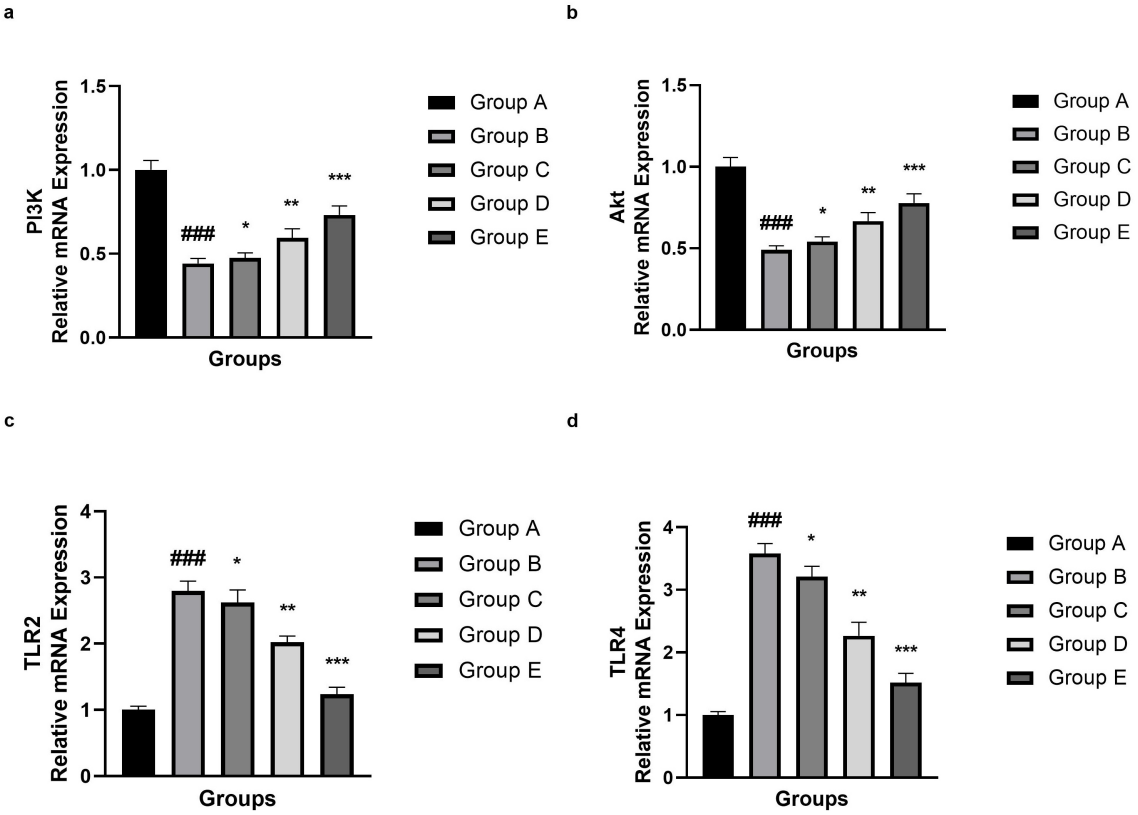

Fig. 11. Effect of umbelliferone on the mRNA expression (PI3K, Akt, TLR2 and TLR) against SAH in mice. (a) PI3K, (b) Akt, (c) TLR2 and (d) TLR4. Data are presented as the mean ± SD, with ten mice in each group. $^{\#\#\#}p < 0.001$ SAH vs normal control; $^{*}p < 0.05$, $^{**}p < 0.01$ and $^{***}p < 0.001$ compared umbelliferone group vs SAH. PI3K, phosphoinositide 3-kinase; AkT, protein kinase B; TLR2, toll-like receptor 2; TLR4, toll-like receptor 4.

groundwork for future preclinical and clinical studies aimed at improving outcomes for patients with this morbid disease [1,3].

Antioxidants such as SOD, CAT, GSH, and GPx form a coordinated defense system against reactive oxygen species (ROS), detoxifying them and thereby protecting against oxidative damage. Redox balance is impaired by a decrease in antioxidant activity or levels, predisposing tissues to oxidative damage and disease progression [22]. Inflammation, which is closely associated with oxidative stress, is a complex network of signaling molecules and transcription factors that controls immune responses. Pro-inflammatory cytokines that induce leukocyte recruitment to the site of injury produce more ROS and initiate apoptotic signaling pathways which can further destroy tissue [1,4,23]. Conversely, anti-inflammatory cytokines such as IL-10 check this response by repressing inflammation signaling and promoting tissue healing. Inflammatory mediators also participate in inflammation spreading and pain sensation, with NF-κB playing a central role as a transcription factor for these pro-inflammatory genes [24,25]. Collectively, these biomarkers provide an overall view of the interaction between oxidative stress and inflammation in pathology.

The pro-inflammatory response significantly contributes to the pathophysiology of EBI after experimental SAH and transcription factor NF-κB has been proposed as a key player in this process. NF-κB activation results in the expression of pro-inflammatory cytokines such as TNF-α and IL-1β, which intensify neuroinflammation and induce neuronal damage. Our finding of an early rise in nuclear NF-κB translocation and increased cytokines at 48 h after SAH implies a strong inflammatory cascade associated with necroptosis activation [26,27]. Necroptosis, which is marked by organelle swelling, plasma membrane rupture and immune cell infiltration, enhances the inflammatory environment and thus exacerbates EBI outcomes [21]. Here, umbelliferone blocks this cascade of events that leads to necroptotic cell death and the liberation of proinflammatory mediators, thereby reducing NF-κB activation and cytokine induction. This bidirectionality restrains inflammation and supports neuronal integrity, suggesting that umbelliferone could be a potential therapeutic strategy for attenuating EBI following SAH. In addition, anti-inflammation of multiple agents has been highly associated with their effectiveness in ameliorating EBI, thus indicating that the protective action of umbelliferone could mainly come from its ability to attenuate necroptosis-mediated neuroinflammation.

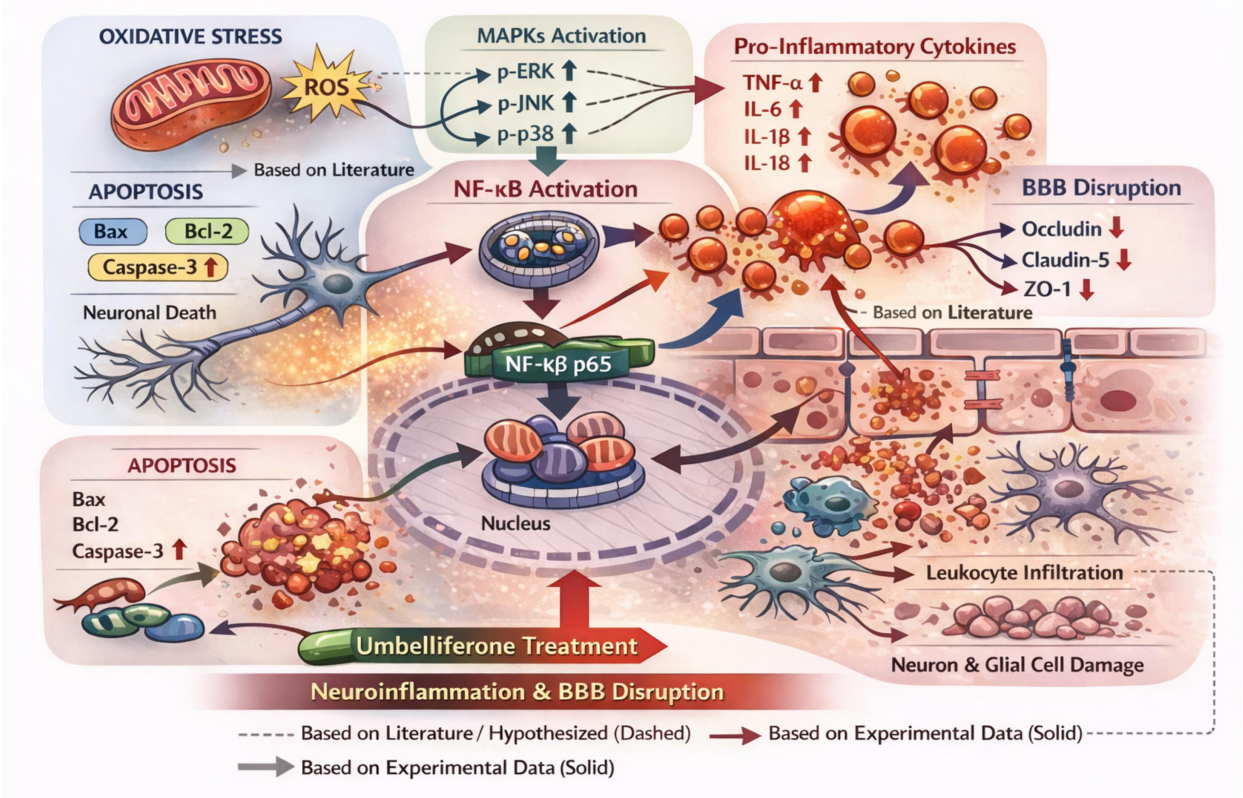

Fig. 12. The mechanism diagram shows that SAH causes excessive oxidative stress, leading to the overproduction of reactive oxygen species (ROS), which activate the MAPK signaling pathway (p-ERK, p-JNK, and p-p38). MAPK activation activates NF-κB p65, which then translocates to the nucleus, where it upregulates the transcription of pro-inflammatory cytokines. This inflammatory environment worsens blood brain barrier (BBB) damage by decreasing tight junction proteins (occludin, claudin-5, ZO-1), leading to leucocyte infiltration and neuroinflammation. Meanwhile, oxidative and inflammatory stress (R)-induced a mitochondria-mediated apoptotic pathway, with increased Bax expression, decreased Bcl-2 levels, and increased caspase-3 activity, resulting in the death of both neurons and glial cells, as demonstrated by current (and previous) data. The pathological events could be ameliorated by UF treatment, which results from the inhibition of ROS production, MAPK and NF-κB activation, decreased release of pro-inflammatory cytokines, maintenance of BBB integrity, and anti-apoptosis, thereby inhibiting neuroinflammation and BBB disruption after SAH.

MMP-9-mediated disruption of the BBB enhances the entry of plasma proteins and immune cells into the brain parenchyma, exacerbating neuroinflammation and leading to vasogenic edema [28,29]. This pathological elevation of vascular permeability exacerbates brain edema, and most importantly, forms the basis for secondary neuronal injuries due to oxidative stress and excitotoxicity. The fact that brain pericytes are a major source of MMP-9 upon thrombin stimulation highlights the complicated crosstalk between the coagulation cascade and NVCU members in the acute phase of an insult to the brain. Pharmacologically, drugs against thrombin can be explored as an effective strategy in reducing MMP-9 induced BBB disruption and edema. Blocking thrombin activity early after injury may downregulate MMP-9 expression in pericytes, thus preventing BBB damage and the consequent entry of detrimental inflammatory mediators. This treatment not only prevents the development of secondary injury cascades (e.g., microglial activation and neuronal apoptosis) but also promotes functional recovery through stabilization of the neurovascular microenvironment [28,30–32]. Elucidation of relationships among thrombin signaling, pericyte activation, and MMP-9 release would provide additional approaches to treat edema associated with a large number of devastating neuropathological conditions, including TBI, stroke, and other ischemic insults. Gaining control over the formation of edema would likely be therapeutic [28,30].

Activation of the PI3K/Akt signaling pathway is associated with increased neuronal survival by blocking apoptotic cascade via effectors including phosphorylation of Bad and caspase-9, which are known to counteract programmed cell death [33,34]. Furthermore, PI3K/Akt signaling also regulates oxidative stress by up-regulating oxidant scavenger molecules and inhibits pro-inflammatory mediators, promoting overall cerebrovascular hemostasis and blood–brain barrier preservation following SAH [34,35]. Blockade of this pathway enhances EBI by promoting neuronal apoptosis, inflammation, and vascular permeability that

contribute to the development of SAH-related neurological deficits. The neuroprotective effects of umbelliferone are associated with the ability to modulate the PI3K/Akt pathway and to leverage its antioxidant and anti-inflammatory properties to prevent damage caused by SAH. Through the mediation of PI3K/Akt activity to restore, umbelliferone eliminates neuronal apoptosis and oxidative damage, providing structural integration as well as functional maintenance for blood–brain barrier integrity, which is essential to protect secondary injurious cascades [33,35,36]. These multi-target effects emphasize umbelliferone's therapeutic potential, not only by targeting molecular signaling pathways but also by ameliorating complex pathophysiological changes following SAH.

Importantly, although current work focuses on the role of TLR2, the contribution of TLR4 as a co-stimulatory receptor for T cell activation has been less investigated. In view of the complex immune environment in the brain, in which cytokines such as IFN-γ and IL-1 play a crucial role in modulating neuroinflammation/immune responses, crosstalk between TLR2 and TLR4 might significantly impact pathology. Exploring their potential synergistic actions will help to uncover new mechanisms regarding neuroimmune modulation following SAH [37,38]. Additionally, the small sample sizes used in these experiments could, to some extent, reduce statistical power and the generalizability of these findings, so future studies should focus on using larger samples to ensure robustness and reproducibility. In addition to neuronal cells, the involvement of glial cells, primarily microglia, is pivotal for the inflammatory environment after SAH [39,40]. The activated microglia which are the CNS resident immune cells, release pro-inflammatory molecules, which further aggravate neuro-injury and induce secondary damaging cascades.

Several studies found similar neuroprotective, antioxidant and anti-inflammatory effects for coumarin derivatives and related phenolic compounds as we have obtained with umbelliferone. For instance, numerous simple coumarins (e.g., esculetin and scopoletin) as well as more complex derivatives (e.g., osthole and daphnetin) have been shown to abrogate oxidative stress, decrease the production of pro-inflammatory cytokines, and restrain apoptotic signaling in models of cerebral ischemia, traumatic brain injury and other acute CNS insults [41]. These compounds frequently modulate shared injury pathways specifically ROS scavenging, inhibition of NF-κB signaling, and repression of MAPK phosphorylation which yield effects overlapping with the decreases in MDA, proinflammatory cytokines, and the ratios of p-ERK/p-JNK/p-p38 we noted following umbelliferone treatment [42]. Emphasizing these commonalities situates our findings within a wider mechanistic framework and strengthens the notion of umbelliferone as a molecular candidate with similar pharmacological potential to other neuroprotective coumarins [43].

5. Limitation

This study is not without its limitations, which the reader should keep in mind when interpreting the results. The experiments were performed in a single mouse model of SAH, and therefore, the findings may not be directly translated to human disease due to species differences in pathophysiology or drug metabolism. Also, the experimental study was confined to short-term biochemical and molecular results and no long-term (neurological, behavioral or cognitive) responses were measured; hence, it is not known whether the demonstrated molecular/cell improvements lead to sustained functional recovery. Although changes in the TLR2/TLR4–NF-κB–MMP-9 and PI3K/Akt signaling pathways were identified, the causative role of these pathways was not confirmed using specific inhibitors or genetic approaches, and the mechanistic implications should be considered associative rather than definitive (Fig. 12). In addition, the pharmacokinetic profiling and brain distribution of umbelliferone were not determined, which limits the interpretation of dose–response relationships and target engagement.

6. Conclusion

The current study demonstrated that umbelliferone has a strong neuroprotective effect on SAH-induced EBI via multiple signaling pathways. The protective effects of umbelliferone against oxidative stress and neuroinflammation were successfully ameliorated, as indicated by the restoration of antioxidant status and inhibition of pro-inflammatory cytokines. At the molecular level, these benefits were associated with inactivation of the TLR2/TLR4–NF-κB–MMP-9 axis to attenuate BBB breakdown and brain edema, as well as activation of the PI3K/Akt survival pathway to suppress neuronal apoptosis. These multi-targeted effects together suggest that umbelliferone is a potential candidate for the treatment of SAH-induced secondary brain injury.

Availability of Data and Materials

The raw data will be available on the request to the corresponding author.

Author Contributions

HZ and XL performed the experimental study. YZ designed the experimental study. HZ draft the manuscript. All authors contributed to editorial changes in the manuscript. All authors read and approved the final manuscript. All authors have participated sufficiently in the work and agreed to be accountable for all aspects of the work.

Ethics Approval and Consent to Participate

The experimental protocols were reviewed and approved by the Animal Ethics Committee of Baotou Central Hospital, China and all procedures were performed under

the approved ethical standards. The ethics approval number is [Approval No. 12783948]. All animal testing follows the 3R principle and the ARRIVE guidelines.

Acknowledgment

Not applicable.

Funding

This research received no external funding.

Conflicts of Interest

The authors declare no conflicts of interest.

Declaration of AI and AI-Assisted Technologies in the Writing Process

During the preparation of this work, the author used the ChatGPT 4 tool to create Figures 1 and 12. After using this tool, the authors reviewed the content as needed and took full responsibility for the content of the publication.

References

[1] Dong H, Gao X, Li H, Gao J, Zhang L. Protective effects of flavonoids against intracerebral and subarachnoid hemorrhage (Review). Experimental and Therapeutic Medicine. 2024; 28: 350. https://doi.org/10.3892/etm.2024.12639.

[2] Ma SJ, Li C, Yan C, Liu N, Jiang GY, Yang HR, *et al*. Melatonin alleviates early brain injury by inhibiting the NRF2-mediated ferroptosis pathway after subarachnoid hemorrhage. Free Radical Biology & Medicine. 2023; 208: 555–570. https://doi.org/10.1016/j.freeradbiomed.2023.09.012.

[3] Zhang ZH, Liu JQ, Hu CD, Zhao XT, Qin FY, Zhuang Z, *et al*. Luteolin Confers Cerebroprotection after Subarachnoid Hemorrhage by Suppression of NLPR3 Inflammasome Activation through Nrf2-Dependent Pathway. Oxidative Medicine and Cellular Longevity. 2021; 2021: 5838101. https://doi.org/10.1155/2021/5838101.

[4] Zolnourian A, Galea I, Bulters D. Neuroprotective Role of the Nrf2 Pathway in Subarachnoid Haemorrhage and Its Therapeutic Potential. Oxidative Medicine and Cellular Longevity. 2019; 2019: 6218239. https://doi.org/10.1155/2019/6218239.

[5] Pugazenthi S, Norris AJ, Lauzier DC, Lele AV, Huguenard A, Dhar R, *et al*. Conditioning-based therapeutics for aneurysmal subarachnoid hemorrhage - A critical review. Journal of Cerebral Blood Flow and Metabolism. 2024; 44: 317–332. https://doi.org/10.1177/0271678X231218908.

[6] Kong D, Guo J, Yang S, Wang X, Guo Q, Ren X, *et al*. Osteopontin inhibitor alleviates neuroinflammation after subarachnoid hemorrhage in rats via TLR4/NF-κB pathway. Brain Research Bulletin. 2025; 232: 111607. https://doi.org/10.1016/j.brainresbull.2025.111607.

[7] Tu T, Yin S, Pang J, Zhang X, Zhang L, Zhang Y, *et al*. Irisin Contributes to Neuroprotection by Promoting Mitochondrial Biogenesis After Experimental Subarachnoid Hemorrhage. Frontiers in Aging Neuroscience. 2021; 13: 640215. https://doi.org/10.3389/fnagi.2021.640215.

[8] Li T, Wang H, Ding Y, Zhou M, Zhou X, Zhang X, *et al*. Genetic elimination of Nrf2 aggravates secondary complications except for vasospasm after experimental subarachnoid hemorrhage in mice. Brain Research. 2014; 1558: 90–99. https://doi.org/10.1016/j.brainres.2014.02.036.

[9] Wang Z, Guo S, Wang J, Shen Y, Zhang J, Wu Q. Nrf2/HO-1 mediates the neuroprotective effect of mangiferin on early brain injury after subarachnoid hemorrhage by attenuating mitochondria-related apoptosis and neuroinflammation. Scientific Reports. 2017; 7: 11883. https://doi.org/10.1038/s41598-017-12160-6.

[10] Zeng Y, Fang Z, Lai J, Wu Z, Lin W, Yao H, *et al*. Activation of Sirtuin-1 by Pinocembrin Treatment Contributes to Reduced Early Brain Injury after Subarachnoid Hemorrhage. Oxidative Medicine and Cellular Longevity. 2022; 2022: 2242833. https://doi.org/10.1155/2022/2242833.

[11] Zhang X, Wu Q, Lu Y, Wan J, Dai H, Zhou X, *et al*. Cerebroprotection by salvianolic acid B after experimental subarachnoid hemorrhage occurs via Nrf2- and SIRT1-dependent pathways. Free Radical Biology & Medicine. 2018; 124: 504–516. https://doi.org/10.1016/j.freeradbiomed.2018.06.035.

[12] Zhang Y, Yang X, Ge X, Zhang F. Puerarin attenuates neurological deficits via Bcl-2/Bax/cleaved caspase-3 and Sirt3/SOD2 apoptotic pathways in subarachnoid hemorrhage mice. Biomedicine & Pharmacotherapy. 2019; 109: 726–733. https://doi.org/10.1016/j.biopha.2018.10.161.

[13] Matsubara H, Imai T, Tsuji S, Oka N, Egashira Y, Enomoto Y, *et al*. Nafamostat protects against early brain injury after subarachnoid hemorrhage in mice. Journal of Pharmacological Sciences. 2022; 148: 65–72. https://doi.org/10.1016/j.jphs.2021.10.007.

[14] Suzuki Y, Nampei M, Kawakita F, Oinaka H, Nakajima H, Suzuki H. The effect of Fibulin-5 on early brain injury after subarachnoid hemorrhage in mice. Neurochemistry International. 2025; 187: 105989. https://doi.org/10.1016/j.neuint.2025.105989.

[15] Wang J, Peng J, Gao L, He J, Lin L, Li JM, *et al*. Olfactory mucosa mesenchymal stem cell-derived exosomes protect against neuroinflammation after subarachnoid hemorrhage by activating mitophagy. The Kaohsiung Journal of Medical Sciences. 2025; 41: e12951. https://doi.org/10.1002/kjm2.12951.

[16] Kornicka A, Balewski Ł, Lahutta M, Kokoszka J. Umbelliferone and Its Synthetic Derivatives as Suitable Molecules for the Development of Agents with Biological Activities: A Review of Their Pharmacological and Therapeutic Potential. Pharmaceuticals. 2023; 16: 1732. https://doi.org/10.3390/ph16121732.

[17] Zhao L, Jin X, Xiong Z, Tang H, Guo H, Ye G, *et al*. The Antivirulence Activity of Umbelliferone and Its Protective Effect against *A. hydrophila*-Infected Grass Carp. International Journal of Molecular Sciences. 2022; 23: 11119. https://doi.org/10.3390/ijms231911119.

[18] Albratty M, Makeen HA. An Umbelliferone-induced Caspase-Mediated Apoptosis in MDA-MB-231 Breast Cancer Cells. Indian Journal of Pharmaceutical Education & Research. 2024; 58: 890–898.

[19] Kim DY, Kang YH, Kang MK. Umbelliferone alleviates impaired wound healing and skin barrier dysfunction in high glucose-exposed dermal fibroblasts and diabetic skins. Journal of Molecular Medicine. 2024; 102: 1457–1470. https://doi.org/10.1007/s00109-024-02491-z.

[20] Garcia JH, Wagner S, Liu KF, Hu XJ. Neurological deficit and extent of neuronal necrosis attributable to middle cerebral artery occlusion in rats. Statistical validation. Stroke. 1995; 26: 627–634. https://doi.org/10.1161/01.str.26.4.627.

[21] Li HW, Lan TJ, Yun CX, Yang KD, Du ZC, Luo XF, *et al*. Mangiferin exerts neuroprotective activity against lead-induced toxicity and oxidative stress via Nrf2 pathway. Chinese Herbal Medicines. 2019; 12: 36–46. https://doi.org/10.1016/j.chmed.2019.12.002.

[22] Chen R, Liu H, Zhang G, Zhang Q, Hua W, Zhang L, *et al*. Antioxidants and the risk of stroke: results from NHANES and two-sample Mendelian randomization study. European Journal

of Medical Research. 2024; 29: 50. https://doi.org/10.1186/s40001-024-01646-5.

[23] Chen W, Zhang HT, Qin SC. Neuroprotective Effects of Molecular Hydrogen: A Critical Review. Neuroscience Bulletin. 2021; 37: 389–404. https://doi.org/10.1007/s12264-020-00597-1.

[24] Xing W, Zhao J, Liu J, Liu Z, Chen G. The protective effects of sevoflurane on subarachnoid hemorrhage. Medical Gas Research. 2024; 14: 1–5. https://doi.org/10.4103/2045-9912.379167.

[25] Teng L, Fan L, Peng Y, He X, Chen H, Duan H, *et al*. Carnosic Acid Mitigates Early Brain Injury After Subarachnoid Hemorrhage: Possible Involvement of the SIRT1/p66shc Signaling Pathway. Frontiers in Neuroscience. 2019; 13: 26. https://doi.org/10.3389/fnins.2019.00026.

[26] Liu M, Jayaraman K, Mehla J, Diwan D, Nelson JW, Hussein AE, *et al*. Isoflurane Conditioning Provides Protection against Subarachnoid Hemorrhage Induced Delayed Cerebral Ischemia through NF-kB Inhibition. Biomedicines. 2023; 11: 1163. https://doi.org/10.3390/biomedicines11041163.

[27] Fu XM, Li CL, Jiang HR, Zhang JY, Sun T, Zhou F. Neuroinflammatory response after subarachnoid hemorrhage: A review of possible treatment targets. Clinical Neurology and Neurosurgery. 2025; 252: 108843. https://doi.org/10.1016/j.clineuro.2025.108843.

[28] Duan HZ, Wu CW, Shen SL, Zhang JY, Li L. Neuroprotective Effects of Early Brain Injury after Subarachnoid Hemorrhage in Rats by Calcium Channel Mediating Hydrogen Sulfide. Cellular and Molecular Neurobiology. 2021; 41: 1707–1714. https://doi.org/10.1007/s10571-020-00940-0.

[29] Horstmann S, Su Y, Koziol J, Meyding-Lamadé U, Nagel S, Wagner S. MMP-2 and MMP-9 levels in peripheral blood after subarachnoid hemorrhage. Journal of the Neurological Sciences. 2006; 251: 82–86. https://doi.org/10.1016/j.jns.2006.09.005.

[30] Li DD, Song JN, An JY, Zhang M, Sun P, Pang HG, *et al*. The trends of peripheral blood leucocyte counts and MMP-9/ TIMP-1 ratio in acute experimental subarachnoid hemorrhage model in rats and their relationship with early brain injury. Journal of Xi'an Jiaotong University (Medical Sciences). 2013; 34: 717. https://doi.org/10.7652/jdyxb201306004. (In Chinese)

[31] Narayan V, Kumar M, Mahajan S, Ganesh V, Luthra A, Gupta T, *et al*. The Role of Serum Matrix Metalloproteinase-9 as a Predictor of Delayed Cerebral Ischemia in Patients with Aneurysmal Subarachnoid Hemorrhage. Journal of Molecular Neuroscience. 2024; 74: 18. https://doi.org/10.1007/s12031-024-02194-7.

[32] Göktürk Y, Gokturk S, Çelik SE. The potential contributions of matrix metalloproteinase 8,9 and 13 (MMP-8,9,13) to cerebral vasospasm and the role of doxycycline inhibitors on gene expression after experimental subarachnoid haemorrhage. Folia Neuropathologica. 2024; 62: 305–311. https://doi.org/10.5114/fn.2024.143698.

[33] Zhang HB, Tu XK, Chen Q, Shi SS. Propofol Reduces Inflammatory Brain Injury after Subarachnoid Hemorrhage: Involvement of PI3K/Akt Pathway. Journal of Stroke and Cerebrovascular Diseases. 2019; 28: 104375. https://doi.org/10.1016/j.jstrokecerebrovasdis.2019.104375.

[34] Hu Q, Li T, Wang L, Xie Y, Liu S, Bai X, *et al*. Neuroprotective Effects of a Smoothened Receptor Agonist against Early Brain Injury after Experimental Subarachnoid Hemorrhage in Rats. Frontiers in Cellular Neuroscience. 2017; 10: 306. https://doi.org/10.3389/fncel.2016.00306.

[35] Gao Y, Ding XS, Xu S, Wang W, Zuo QL, Kuai F. Neuroprotective effects of edaravone on early brain injury in rats after subarachnoid hemorrhage. Chinese Medical Journal. 2009; 122: 1935–1940.

[36] Tang H, Shao C, Wang X, Cao Y, Li Z, Luo X, *et al*. 6-Gingerol attenuates subarachnoid hemorrhage-induced early brain injury via GBP2/PI3K/AKT pathway in the rat model. Frontiers in Pharmacology. 2022; 13: 882121. https://doi.org/10.3389/fphar.2022.882121.

[37] Heinz R, Schneider UC. TLR4-Pathway-Associated Biomarkers in Subarachnoid Hemorrhage (SAH): Potential Targets for Future Anti-Inflammatory Therapies. International Journal of Molecular Sciences. 2022; 23: 12618. https://doi.org/10.3390/ijms232012618.

[38] Xu YP, Tao YN, Wu YP, Zhang J, Jiao W, Wang YH, *et al*. Sleep deprivation aggravates brain injury after experimental subarachnoid hemorrhage via TLR4-MyD88 pathway. Aging. 2021; 13: 3101–3111. https://doi.org/10.18632/aging.202503.

[39] Hanafy KA. The role of microglia and the TLR4 pathway in neuronal apoptosis and vasospasm after subarachnoid hemorrhage. Journal of Neuroinflammation. 2013; 10: 83. https://doi.org/10.1186/1742-2094-10-83.

[40] Hu ZQ, Ma R, Sun JQ, Peng M, Yuan J, Lai N, *et al*. Tenascin-C Facilitates Microglial Polarization via TLR4/MyD88/NF-κB Pathway Following Subarachnoid Hemorrhage. Journal of Inflammation Research. 2025; 18: 3555–3570. https://doi.org/10.2147/JIR.S511378.

[41] Flores-Morales V, Villasana-Ruíz AP, Garza-Veloz I, González-Delgado S, Martinez-Fierro ML. Therapeutic Effects of Coumarins with Different Substitution Patterns. Molecules. 2023; 28: 2413. https://doi.org/10.3390/molecules28052413.

[42] Chistyakov DV, Nikolskaya AI, Gorbatenko VO, Goriainov SV, Silachev DN, Sergeeva MG. Inhibitor of hyaluronic acid synthesis 4-methylumbelliferone (4-MU) as a potential anti-inflammatory substance in acute neuroinflammation model in vivo. Inflammopharmacology. 2026; 34: 485–494. https://doi.org/10.1007/s10787-025-02063-8.

[43] Peng Y, Jin J, Fan L, Xu H, He P, Li J, *et al*. Rolipram Attenuates Early Brain Injury Following Experimental Subarachnoid Hemorrhage in Rats: Possibly via Regulating the SIRT1/NF-κB Pathway. Neurochemical Research. 2018; 43: 785–795. https://doi.org/10.1007/s11064-018-2480-4.